KSCE Journal of Civil Engineering (2021) 25(7):2725-2736
DOI 10.1007/s12205-021-0755-9

pISSN 1226-7988, eISSN 1976-3808
www.springer.com/12205

Tunnel Engineering

Theoretical Method of Chamber Pressure for EPB Shield Tunneling Under-Crossing Existing Metro Tunnels

Hongpeng Lai[a], Tengteng Wang[a], Zuo Kang[b], Rui Chen[a], and Qiuyang Hong[a]

[a]*School of Highway, Chang'an University, Xi'an 710064, China*
[b]*Xi'an Mass Transit Railway Co., Ltd., Xi'an 710016, China*

ARTICLE HISTORY

Received 25 April 2020
Revised 6 January 2021
Accepted 31 January 2021
Published Online 2 April 2021

KEYWORDS

Tunnel engineering
Earth pressure balance shield (EPB)
Chamber pressure
Under-crossing tunnel

ABSTRACT

As an increasing number of metro lines have been planned or executed in urban area, new tunnel undercrossing existing tunnels has been commonly practiced. Construction of the existing tunnel causes disturbance to the surrounding soil and hence affects the operational parameters of undercrossing tunneling especially the chamber pressure of EPB machine. However, very limited research studies this effect. To fill the gap of knowledge, this paper proposed a new method for calculating the chamber pressure of EPB tunneling machine in undercrossing project. First, the effect of existing tunnel on surrounding soil is classified as removal-and-replacement effect, excavation-induced-disturbance effect, and elastic foundation beam effect. Second, based on analysis of the mutual interaction between existing tunnel and the undercrossing tunneling, three zones have been identified to study the chamber pressure of EPB machine. Next, a new method is proposed to calculate the chamber pressure in the process of undercrossing existing tunnel. Finally, the proposed method has been verified with measured data from two engineering cases. The comparison results show that the proposed method is in good agreement with the measured data, indicating that it is reasonable with high accuracy.

1. Introduction

The congestion of ground traffic has increasingly become a headache for metropolis. The most effective way to solve this problem is to develop underground space and build underground transportation system. To date, 185 metro lines with a total mileage of 5,377 km have been in operation in 35 cities in mainland China. The earth pressure balance (EPB) shield machine is commonly used to construct subway in China due to its advantages of safety and efficiency. With the increase in density of subway lines, more and more shield tunnels are designed or being executed to under pass or over cross the existing tunnels (Chen et al., 2011, 2013, 2018; Li and Chen, 2012; Zhang et al., 2013; Zheng et al., 2015; Goh et al., 2016; Shi et al., 2016; Cheng et al., 2019). In these cases, the construction of undercrossing or overcrossing tunnel will inevitably affect the structure of the existing tunnels. Therefore, the impact on the existing tunnel due to construction of the new shield tunnel must be minimized.

To date, researchers have used different methods to study the effects of nearby tunneling on existing tunnels, including numerical simulation (Chakeri et al., 2011; Zhang and Huang, 2014; Avgerinos et al., 2017; Chen et al., 2019; Liu and Lai, 2019), theoretical analysis (Lai et al., 2017), in-situ monitoring (Li and Yuan, 2012) and model testing (Kim et al., 1998; Byun et al., 2006). Yin et al. (2018) investigated the effect of excavation clearance of the EPB shield and the influence of Mid-shield-grouting (MSG) method on settlement of existing tunnels by 3D finite element method (FEM). Lin et al. (2019) studied the deformation and stress redistribution of existing tunnel caused by obliquely under-crossing new twin tunnels based on numerical simulation. Jin et al. (2018) analyzed the deformation characteristics of the existing tunnel and ground surface due to construction of under-crossing shield tunnel, and they proposed a new empirical formula for predicting the settlement of the existing tunnel based on a large amount of monitoring data collected from 18 engineering cases in Shenzhen, China. In construction of the under-crossing EPB shield tunnel, the stability of excavation face is one of the critical factors to reduce the stratum disturbance and ensure the safety of the existing tunnel (Zhang el al., 2015; Li et al., 2019a, 2019b, 2021; Zheng et al., 2021). Li and Zhang (2020) studied the

CORRESPONDENCE Hongpeng Lai laihp168@chd.edu.cn School of Highway, Chang'an University, Xi'an 710064, China

stability of shield tunnel face in anisotropic sand based on the upper theorem of limit analysis. Li et al. (2019c) investigated the face stability of a shallow tunnel in saturated and multi-layered soils using theoretical analysis and numerical simulation. Wan et al. (2019) proposed a new calculation model of loose earth pressure considering the soil arching effect during the excavation of deep buried tunnel to compute the limit support pressure on tunnel face. Zhang el al. (2020) proposed an improved velocity field for a horseshoe-shaped shield tunnel based on the kinematic approach of limit analysis. The chamber pressure is an important EPB shield construction parameter that balances the water and soil pressure and maintains the stability of the excavation face, and its reasonable value determines the safety of the ground and the existing subway structure when the EPB shield passes through.

The current research is mainly focus on the impact of new tunnels on existing tunnels. However, a large number of measured data show that the earth pressure on EPB shield machine will be reduced when it passes through the existing tunnel (Liao et al., 2005; Ma et al., 2016; Zhang et al., 2016), which means that the presence of the existing tunnel also exerts an impact on new tunneling, especially the chamber pressure. However, there is very limited research studying the effect of existing tunnel on the operation parameters of EPB shield tunneling, especially on the chamber pressure. To fill this gap of knowledge, in this paper, the influence of the new tunnel and the existing tunnel on the surrounding soil is studied to determine the reasonable chamber pressure. Firstly, the interaction between the existing tunnel and new tunnel is explored. This interaction is transferred by the surrounding soil, and hence the effect of existing tunnel on surrounding soil must be clarified. The effects of existing tunnel on surrounding soil are divided into removal-and-replacement effect, excavation-induced-disturbance effect and elastic foundation beam effect. The Mindlin solution is used to study the mechanical behavior of the existing tunnel caused by construction of new shield tunnel. Next, the interaction between the under-crossing shield crossing and the existing tunnel is divided into three types of influence zone. Finally, based on the types of influence zone, the paper deduces equations for calculating the chamber pressure of EPB machine during undercrossing process and verified the calculated results with measured data.

2. Analysis of the Interaction of Shield Tunneling Under-Crossing Existing Tunnel

The process of shield tunnelling under-crossing existing tunnel involves the interactions among the shield tunnel, the existing tunnel and the surrounding soil. As an important medium, the surrounding soil not only affects the deformation of the existing tunnel but also determines the construction parameters of the new shield tunnel, especially the chamber pressure. Construction of shield tunnel changes the stress field of surrounding soil, resulting in deformation and additional stress on existing tunnel (Fang et al., 2014), and the existence of existing tunnel will also

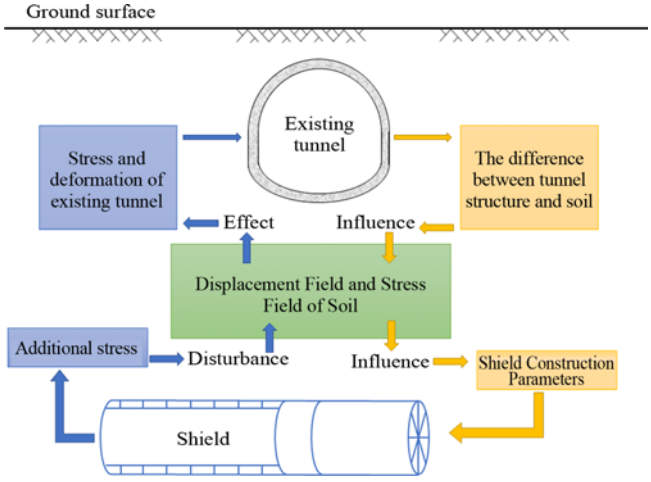

Fig. 1. Diagram of Interaction between Shield Tunnels and Existing Tunnels

affect the stress-strain behavior the surrounding soil because of the differences between tunnel structure and surrounding soil in stiffness, modulus of elasticity, material properties, etc., which in return will affect the construction of shield tunnel. This idea is presented in the Fig. 1.

2.1 Influence of Existing Tunnel on the New Tunnel and Surrounding Soil

Previous studies have shown that the presence of structures can

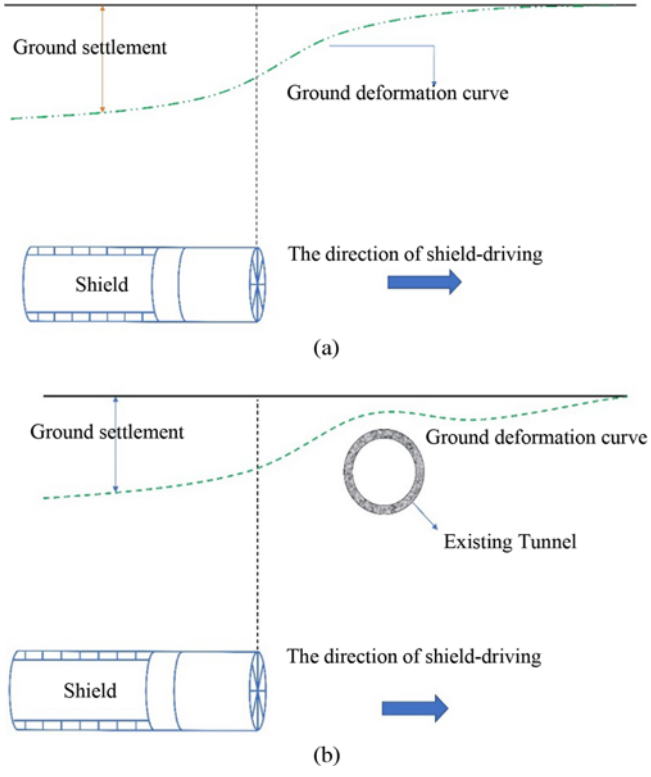

Fig. 2. Schematic Diagram of Soil Deformation in the Presence or Absence of Existing Tunnels: (a) Soil Deformation in the Presence of Existing Tunnels, (b) Soil Deformation without Existing Tunnels

change the deformation pattern of the soil as shown in Fig. 2 (Dimmock and Mair, 2008; Maleki et al., 2011; Twana et al., 2018). The influence of the existing tunnel on the soil is classified as follows: 1) Removal-and-replacement effect: due to excavation of the soil and replacement it by tunnel structure leading to change of the stress field. 2) Excavation-induced-disturbance effect: construction of the existing tunnel will disturb the surrounding soil to a certain range, which will affect the distribution of earth pressure on the EPB machine and therefore the operating parameters (chamber pressure) need to be adjusted when the shield machine under-crosses. 3) Effect of elastic foundation beam: the existing tunnel has large rigidity, the effect of which is similar to the reinforcement of soil, and for the under-crossing tunnel this means part of the earth pressure will be shared by the existing tunnel during construction.

2.1.1 The Removal-and-Replacement Effect

Figure 3 shows the removal-and-replacement effect of existing tunnel on shield tunneling, and the following assumptions are made: 1) the influence of the longitudinal slope on the earth pressure is ignored; 2) the existing tunnel is regarded as a hollow cylinder with an inner diameter of R_1 and an outer diameter of R, and the thickness of lining is d.

When $x' < R$, where x' is measured from the projected intersection line between the existing tunnel and the advancing cutter head, as shown in Fig. 3.

The projected area and height of the displaced soil may be expressed as

$$S_1 = arc\cos\left(1-\frac{x'}{R_1}\right)*R_1^2*\left[1-\sqrt{1-\left(1-\frac{x'}{R_1}\right)^2}\right], \tag{1}$$

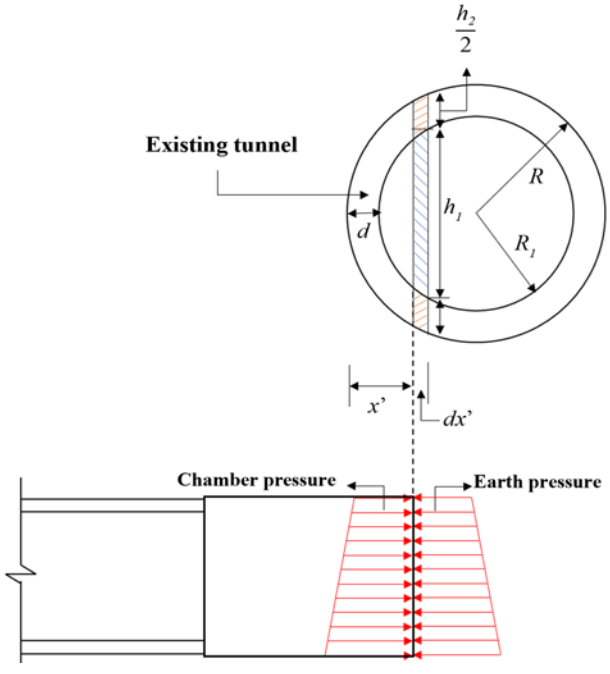

Fig. 3. Schematic Diagram of Displacement Soil

$$h_1 = 2R_1\sin\left(arc\cos\frac{R-x'}{R_1}\right) = 2\sqrt{R_1^2-(R-x')^2}. \tag{2}$$

And the projected height of the existing structure may be expressed as

$$h_2 = 2R\sin\left(arc\cos\frac{R-x'}{R}\right)-h_1 = 2\sqrt{2Rx'-x'^2}-2\sqrt{R_1^2-(R-x')^2}. \tag{3}$$

When $x' \geq R$, the projected area and height formula of the displaced soil may be expressed as

$$S_2 = \pi R_1^2 - arc\cos\left(-1+\frac{x'}{R_1}\right)*R_1^2*\left[1-\sqrt{1-\left(-1+\frac{x'}{R_1}\right)^2}\right], \tag{4}$$

$$h_1 = 2R_1\sin\left(arc\cos\frac{x'-R}{R_1}\right). \tag{5}$$

And the projected height of the existing structure may be expressed as

$$h_2 = 2R\sin\left(arc\cos\frac{x'-R}{R}\right)-h_1. \tag{6}$$

The overburden pressures at the base of existing tunnel before and after the excavation of soil are respectively

$$p_1 = \gamma_1(h_1+h_2), \tag{7}$$

$$p_2 = \gamma_2 h_2, \tag{8}$$

where γ_1 is the average unit weight of the excavated soil; γ_2 is the unit weight of reinforced concrete of existing tunnel.

Since the removal-and-replacement action is to remove the soil and replace it with the lining structure, the net overburden pressure can be expressed as

$$p_{re} = p_1 - p_2. \tag{9}$$

2.1.2 The Excavation-Induced-Disturbance Effect

Excavation of the existing tunnel has caused the redistribution of stress in surrounding soil. In this paper, the following assumptions are made: 1) the impact of the excavation on the surrounding soil decreases with distance in space. Therefore, it is assumed that the excavation affected area is 3 times the tunnel diameter; 2) tunnel excavation is instantaneous unloading, and the lining is treated as concrete to replace the surrounding soil of the corresponding part; 3) this problem is simplified as a plane strain problem in polar coordinate.

After construction of the tunnel structure, the numerical model is shown in Fig. 4 and the equilibrium equations, geometric equations and physical equations of the model based on elasticity theory are as follows:

$$\left.\begin{aligned}&\frac{\partial\sigma_r}{\partial r}+\frac{1}{r}\frac{\partial\tau_{r\varphi}}{\partial\varphi}+\frac{\sigma_r-\sigma_\varphi}{r}+f_r=0\\&\frac{1}{r}\frac{\partial\sigma_\varphi}{\partial\varphi}+\frac{\partial\tau_{r\varphi}}{\partial r}+\frac{2\tau_{r\varphi}}{r}+f_\varphi=0\end{aligned}\right\}, \tag{10}$$

$$\left.\begin{aligned}\varepsilon_r &= \frac{\partial u_r}{\partial r}\\ \varepsilon_\varphi &= \frac{u_r}{r}+\frac{1}{r}\frac{\partial u_\varphi}{\partial \varphi}\\ \gamma_{r\varphi} &= \frac{1}{r}\frac{\partial u_r}{\partial \varphi}+\frac{\partial u_\varphi}{\partial r}-\frac{u_\varphi}{r}\end{aligned}\right\}, \tag{11}$$

$$\left.\begin{aligned}\varepsilon_r &= \frac{1-\mu^2}{E_s}\left(\sigma_r-\frac{1-\mu}{\mu}\sigma_\varphi\right)\\ \varepsilon_\varphi &= \frac{1-\mu^2}{E_s}\left(\sigma_\varphi-\frac{1-\mu}{\mu}\sigma_r\right)\\ \gamma_{r\varphi} &= \frac{2(1+\mu)}{E_s}\tau_{r\varphi}\end{aligned}\right\}. \tag{12}$$

The boundary conditions according to Fig. 4 are as follows:

$$\left.\begin{aligned}P &= \int\gamma(z)dz\\ Q &= K_0\int\gamma(z)dz\\ \tau_{zx} &= 0\end{aligned}\right\}, \tag{13}$$

$$\left.\begin{aligned}\sigma_r &= \frac{1}{2}(P+Q)-\frac{1}{2}(P-Q)\cos 2\varphi\\ \sigma_\varphi &= \frac{1}{2}(P+Q)+\frac{1}{2}(P-Q)\cos 2\varphi\\ \tau_{r\varphi} &= \frac{1}{2}(P-Q)\sin 2\varphi\end{aligned}\right\}, \tag{14}$$

where P is vertical self-weight stress; Q lateral stress; σ_r is normal stress in radial direction in polar coordinate; σ_φ is normal stress in circumferential direction in polar coordinates; $\tau_{r\varphi}$ is shear stress in polar coordinates; ε_r and ε_φ are corresponding normal strains in radial and circumferential directions; $\gamma_{r\varphi}$ is shear strain; E_s is the elastic modulus of the soil below the existing tunnel; K_0 is coefficient of earth pressure at rest.

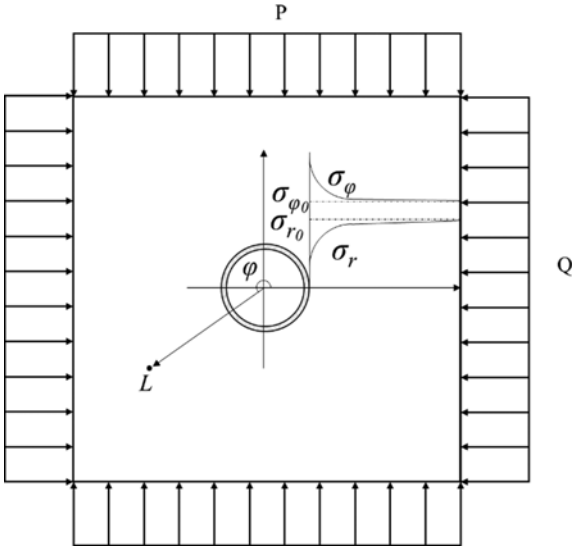

Fig. 4. Elastic Mechanics Solution Model for Existing Tunnel Excavation and Support

In addition, according to boundary conditions, the stress components at a distance L from the origin after tunnel excavation and support can be obtained using the elastic resistance method:

$$\left.\begin{aligned}\sigma_r &= \frac{1}{2}(P+Q)\left(1-\frac{D^2}{L^2}\right)+\frac{D^2}{L^2}S_0-S_n\left(\frac{D^4}{L^4}-\frac{2D^2}{L^2}\right)\cos(2\theta)\\ &\quad\left(-\frac{1}{2}(P-Q)\left(1+\frac{3D^4}{L^4}+\frac{4D^2}{L^2}\right)\cos 2\varphi\right)\\ \sigma_\varphi &= \frac{1}{2}(P+Q)\left(1+\frac{D^2}{L^2}\right)-\frac{D^2}{L^2}S_0+\frac{1}{2}(P-Q)\left(1+\frac{3D^4}{L^4}\right)\cos 2\varphi\\ &\quad+S_n\frac{D^4}{L^4}\cos 2\varphi\\ \tau_{r\varphi} &= \frac{1}{2}(P-Q)\left(1-\frac{3D^4}{L^4}+\frac{2D^2}{L^2}\right)\sin 2\varphi-S_n\left(\frac{D^4}{L^4}-\frac{D^2}{L^2}\right)\sin 2\varphi\end{aligned}\right\}, \tag{15}$$

$$S_0 = \frac{(1+\mu)dE(P+Q)}{2(1+\mu)dE+(1-\mu_E)DE_s}, \tag{16}$$

$$S_n = \frac{3(3-4\mu)(P-Q)}{2\left[5-6\mu+4\dfrac{D^3E_s}{12(1+\mu)EI}\right]}, \tag{17}$$

where S_0 is uniform resistance; S_n is the maximum amplitude of the changing resistance; E is elastic modulus of existing tunnel structure, μ is Poisson's ratio of soil; L is the distance between the desired point and the center of the existing tunnel.

Therefore, the stress field in the surrounding soil after excavation of the existing structure can be expressed as

$$\sigma_x = \frac{1}{2}(\sigma_r+\sigma_\varphi)+\frac{1}{2}(\sigma_r+\sigma_\varphi)\cos 2\varphi-\tau_{r\varphi}\sin 2\varphi, \tag{18}$$

$$\sigma_z = \frac{1}{2}(\sigma_r+\sigma_\varphi)-\frac{1}{2}(\sigma_r+\sigma_\varphi)\cos 2\varphi+\tau_{r\theta}\sin 2\varphi. \tag{19}$$

2.1.3 The Elastic Foundation Beam Effect

As mentioned above, because the elastic modulus of the lining of existing tunnel far outweighs that of soil mass, indicating that part of the earth pressure that is carried by the existing tunnels and hence resulting in the reduction of earth pressure. This is termed as the elastic foundation beam effect of the existing tunnel, which represents the reinforcing effect due to construction of the existing tunnel in the stratum.

According to the Winkler elastic foundation beam theory, the relationship between the vertical deformation Δ at any point at the bottom of the existing tunnel and the vertical earth pressure $p\Delta$ may be expressed as follows:

$$p\Delta = k\Delta. \tag{20}$$

It is assumed that the tunnel and soil deform harmoniously, and the stress change due to Δ is $p\Delta$. The formula for calculating the reduction factor of earth pressure by elastic foundation beam may be expressed as

$$v = p'_{e1}/p_{e1} = (p_{e1}+k\Delta)/p_{e1}. \tag{21}$$

It should be noted that since shield construction may cause settlement or uplift of existing tunnel, so the value of Δ should be marked with a plus or minus sign to clarify the settlement or uplift effect. If the existing tunnel is uplifted, p'_{e1} is smaller than the original earth pressure p_{e1}, so Δ should be a negative value. Similarly, if the existing tunnel is settled, Δ should be a positive value. In view of this, the change of earth pressure caused by the removal-and-replacement effect should also be affected by the effect of elastic foundation beam. Therefore, the calculation formula of earth pressure at the bottom of tunnel under the influence of two factors may be expressed as

$$p_{e1} = v(p_{e0} - p_{re}) . \tag{22}$$

2.2 Impact of New Tunnel on the Existing Tunnel and Surrounding Soil

2.2.1 Calculation of Stress Increase Caused by Shield Construction Based on the Mindlin Solution

The stress increase in the soil under the action of horizontal concentrated force P can be obtained by the Mindlin solution (Mindlin, 1936):

$$\sigma_x = (x,y,z) = \frac{P_x}{2\pi(1-\mu)}\left\{\frac{1-2\mu}{R_1^3} - \frac{(1-2\mu)(5-4\mu)}{R_2^3} + \frac{3x^2}{R_1^5} + \frac{3(3-4\mu)x^2}{R_2^5} + \frac{4(1-\mu)(1-2\mu)}{(R_2R_2+z+c)^2} + \left[3 - \frac{x^2(3R_2+z+c)}{R_2^2(R_2+z+c)}\right] - \frac{6c}{R_2^5}\left[3c-(3-2\mu)(z+c)+\frac{5x^2z}{R_2^2}\right]\right\}, \tag{23}$$

$$\sigma_y = g(x,y,z) = \frac{Px}{8\pi(1-\mu)}\left\{\frac{1-\mu}{R_1^3} - \frac{(1-2\mu)(5-4\mu)}{R_2^3} + \frac{3x^2}{R_1^5} + \frac{3(3-4\mu)y^2}{R_2^5} + \frac{4(1-\mu)(1-2\mu)}{R_2(R_2+z+c)^2}\left[3 - \frac{y^2(3R_2+z+c)}{R_2^2(R_2+z+c)}\right] - \frac{6c}{R_2^5}\left[3c-(3-2\mu)(z+c)+\frac{5y^2z}{R_2^2}\right]\right\}, \tag{24}$$

$$\sigma_z = h(x,y,z) = \frac{Px}{8\pi(1-\mu)}\left\{-\frac{1-2\mu}{R_1^3} + \frac{(1-2\mu)}{R_2^3} + \frac{3(z-c)^2}{R_1^5} + \frac{3(3-4\mu)(z+c)^2}{R_2^5} - \frac{6c}{R_2^5}\left[c+(1-2\mu)(z+c)+\frac{5(z+c^2)z}{R_2^2}\right]\right\}, \tag{25}$$

$$R_1 = \sqrt{x^2+y^2+(z-c)^2} , \tag{26}$$

$$R_2 = \sqrt{x^2+y^2+(z+c)^2} , \tag{27}$$

where x, y are the distances between the calculated point and the force application point in the corresponding coordinate axis, z is buried depth of the calculated point, and c is vertical coordinate of the point of application.

During the construction of the shield tunnel, the additional thrust of the cutter-head q acts on the excavation surface, and the frictional force F_f is assumed to be evenly distributed along the shield shell. These two forces will generate additional stress, which acts on the existing tunnel and causes structural deformation as shown in Fig. 5.

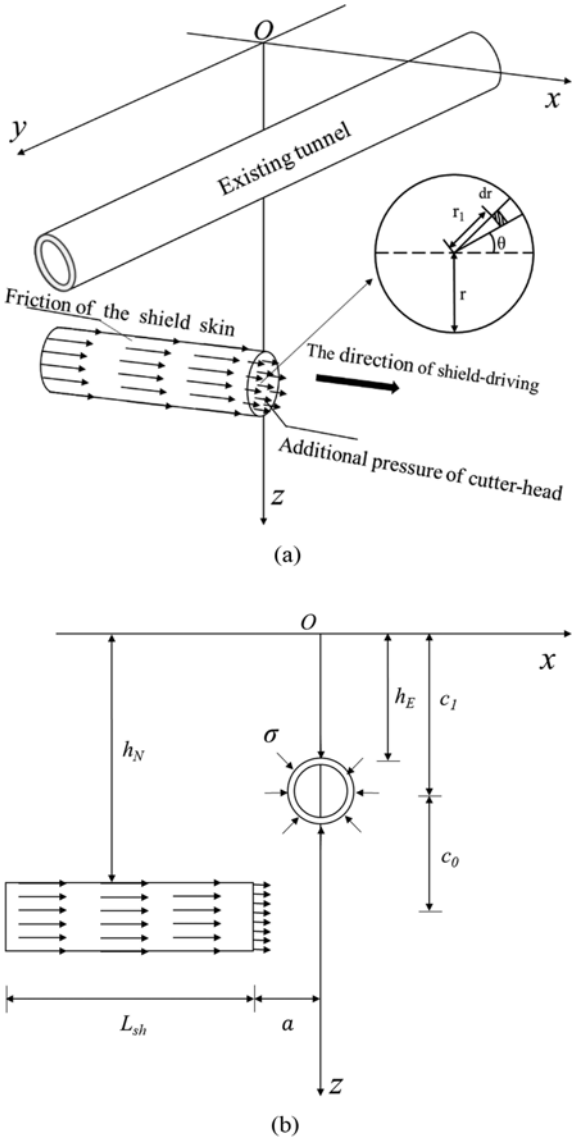

Fig. 5. Schematic Diagram of Mechanical Modela: (a) Schematic Diagram of the Overall Mechanics Model, (b) Sectional View along the Direction of Shield Tunneling

The following assumptions are made:

1) The shield tunnel is advanced horizontally; 2) the additional thrust q is approximately circular uniform load, acting before the cutter head (Shi et al., 2017); 3) friction between the shield shell and surrounding soil F_f is evenly distributed along the shield shell; 4) the consolidation settlement of soil during and after shield construction is neglected.

In previous studies, the disturbance of shield excavation on the existing structure is simplified as the stress increase at the axis of the existing tunnel, and very few studies consider the

stress increase on the whole structure. In this study, the existing structure is regarded as a hollow cylinder with an outer diameter of R and the lining with thickness d as shown in Fig. 5. Based on the Mindlin solution, the stress around the existing tunnel under the influence undercrossing shield tunnel can be obtained.

2.2.1.1 Additional Thrust q

As shown in Fig. 5, the differential area $r_1 dr_1 d\theta$ is taken from the excavation face; the load is $q_1 r_1 dr_1 d\theta$, where q_1 is additional thrust concentration; $x = a - R\cos\delta$, $y = r_1\cos\theta$, $z = R\sin\delta + c_1$, $c = r\sin\theta + c_1 + c_0$. Introducing the above parameters into Eqs. (25) – (27), the vertical additional stress of the soil around the existing tunnel caused by the additional thrust q of can be obtained as follows:

$$d\sigma_{z1} = q_1 r_1 d\theta dr_1 \frac{a - R\cos\delta}{2\pi(1-\mu)}\left\{-\frac{1-2\mu}{R_1^3} + \frac{(1-2\mu)}{R_2^3} + \frac{3(z-c)^2}{R_1^5} + \frac{3(3-4\mu)(z+c)^2}{R_2^5} - \frac{6c}{R_2^5}\left[c + (1-2\mu)(z+c) + \frac{5(z+c)^2 z}{R_2^2}\right]\right\}, \quad (28)$$

$$R_1 = \sqrt{(a - R\cos\delta)^2 + (r_1\cos\theta)^2 + (R\sin\delta - r\sin\theta - c_0)^2}, \quad (29)$$

$$R_2 = \sqrt{(a - R\cos\delta)^2 + (r_1\cos\theta)^2 + (R\sin\delta + r\sin\theta + c_0 + 2c_1)^2}, \quad (30)$$

where R is the radius of the existing tunnel; r is the radius of shield; r_1 is the distance between the additional thrust of the shield and the center point; δ is the angle corresponding to the stress point of the existing tunnel; θ is the angle corresponding to the point of action of the additional thrust; c_0 is the distance between axis of built structure and new tunnel; c_1 is the distance between the axis of the tunnel and the surface of the earth; a the distance between the tunnel axis and the shield cutter-head; based on the load influence range; h_E is buried depth of existing tunnel; h_N is buried depth of new tunnel.

2.2.1.2 Frictional Force F_f

The friction between the EPB shield machine and surrounding soil can usually be obtained by multiplying the earth pressure on the shield surface by the friction coefficient. As shown in Fig. 6, the lateral earth pressure on the left and right sides of the shield is symmetrical, so when calculating the positive pressure generated by the lateral earth pressure on the outer surface of the shield, only $\theta = -\pi/2 - \pi/2$ is considered. The vertical earth pressure of the shield is symmetrical, so when calculating the vertical pressure generated by the vertical earth pressure per unit length, it is only considered $\theta = -\pi/2 - \pi/2$.

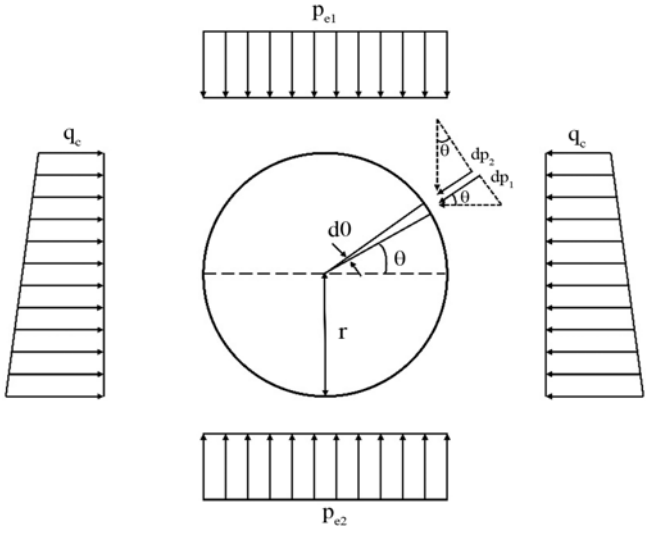

Fig. 6. Calculation Model of Earth Pressure around Shield

P_1 and P_2 are the supporting force per unit length caused by the lateral and vertical earth pressure of the shield respectively, and the calculation formula are

$$P_1 = \int dP_1 = 2\int_{-\frac{\pi}{2}}^{\frac{\pi}{2}} q_e \cos\theta r d\theta = 4 q_e r, \quad (31)$$

$$P_2 = \int dP_2 = 2\int_{-\frac{\pi}{2}}^{0} [p_{e2} - \gamma r(1-\sin\theta)](-\sin\theta) r d\theta + 2\int_{0}^{\frac{\pi}{2}} [p_{e1} + \gamma r(1-\sin\theta)]\sin\theta r d\theta = 2(p_{e1} + p_{e2})r - \pi\gamma r^2, \quad (32)$$

$$p_{e1} = \sum \gamma_i h_i + \gamma_w h_w, \quad (33)$$

$$p_{e2} = p_{e1} + p_g = p_{e1} + \frac{2W}{\pi r l_{sh}}, \quad (34)$$

$$q_e = K_0 p_e, \quad (35)$$

where η is the coefficient of friction between the outer surface of the shield and the excavated soil; p_{e1} is the earth pressure at the top of the shield; p_{e2} is the earth pressure at the bottom of the shield; q_e is the lateral pressure of the shield, calculated by the product of the lateral pressure coefficient K_0 and the vertical earth pressure, W is the weight of the shield machine, l_{sh} is the length of shield machine.

The formula of friction resistance between shield and surrounding soil may be determined as

$$dF_f = \eta(P_1 + P_2) dl_{sh}. \quad (36)$$

Similarly, substituting parameter $x = a + l_{sh} - R\cos\delta$, $y = r\cos\theta$, $z = R\sin\delta + c_1$, $c = r\sin\theta + c_1 + c_0$ into Eqs. (25) – (27), the internal force of the existing tunnel due to friction force can be obtained as

$$d\sigma_{z2} = \eta(P_1 + P_2) dl_{sh} \frac{a - R\cos\delta + l_{sh}}{8\pi(1-\mu)}\left\{-\frac{1-2\mu}{R_1^3} + \frac{(1-2\mu)}{R_2^3} + \frac{3(z-c)^2}{R_1^5} - \frac{3(3-4\mu)(z+c)^2}{R_2^5} - \frac{6c}{R_2^5}\left[c + (1-2\mu)(z+c) + \frac{4(z+c^2)z}{R_2^2}\right]\right\}. \quad (37)$$

2.2.2 Equations for Deformation of Existing Tunnel Caused by Shield Tunnel Construction Based on Elastic Foundation Beam Theory

The additional stress generated by construction of the shield tunnel acts on the existing tunnel and the surrounding soil, causing structural deformation. This effect can be regarded as the

reaction of Winkler elastic foundation beam under distributed load (Yu et al., 2013; Huang et al., 2019; Liu et al., 2019).

The total vertical additional stress generated by shield tunneling on existing tunnels may be expressed by the following equation:

$$d\sigma_z = d\sigma_{z1} + d\sigma_{z2}\,. \tag{38}$$

The value of the base bed coefficient k in the Winkler foundation model is critical. In this paper, Vesic's improved Biot foundation bed coefficient formula is used in this study (Vesic, 1961; Liu et al., 2019):

$$k = \frac{0.65E_s}{1-\mu^2}\left[\frac{E_s D}{EI}\right]^{\frac{1}{12}}, \tag{39}$$

where E_s is the elastic modulus of the soil; E is elastic modulus of existing tunnel structure; D is the width of the elastic foundation, which is the outer diameter of built tunnel; I is moment of inertia, which can be obtained using the formula for calculating the moment of inertia of the circular section.

According to the Winkler foundation beam theory, the differential equation of elastic foundation beam under full span distributed load can be obtained as follows:

$$EI\frac{d^4\Delta}{dx^4} + k\Delta = \int d\sigma_z D\,, \tag{40}$$

where k is coefficient of subgrade bed of soil at the bottom of existing tunnel.

The flexibility characteristic value λ of the elastic foundation beam can be obtained as

$$\lambda = \left(\frac{kB}{4EI}\right)^{0.25}. \tag{41}$$

Combined with the boundary conditions, the displacement $\Delta(\alpha)$ of any point α on the tunnel caused by this load can be obtained as

$$d\Delta(\alpha) = \frac{\sigma_z(\xi)D}{8EI\lambda^3}e^{-\lambda|\alpha-\xi|}(\cos\lambda|\alpha-\xi| + \sin\lambda|\alpha-\xi|)d\xi\,, \tag{42}$$

$$\Delta(\alpha) = \frac{D}{8EI\lambda^3}\int_{-\infty}^{+\infty}\sigma_z(\xi)e^{-\lambda|\alpha-\xi|}(\cos\lambda|\alpha-\xi| + \sin\lambda|\alpha-\xi|)d\xi\,. \tag{43}$$

3. Determination of Chamber Pressure in Different Sections

This paper proposes a method for determining chamber pressure for advancing the EPB shield machine undercrossing the existing tunnel. When the shield machine is advanced to a certain section, based on the Mindlin theory solution, the deformation of the existing structure and the soil can be deduced from resultant effect of the new tunnel. And then, considering the removal-and-replacement, excavation-induced-disturbance and elastic foundation beam effects, chamber pressure in different interaction zone can be determined. On this basis, the change of chamber pressure of EPB shield is determined to ensure that the supporting force provided by the cutter head is not much different from the earth pressure in front, so as to avoid the soil from being squeezed or collapse due to the insufficient supporting force.

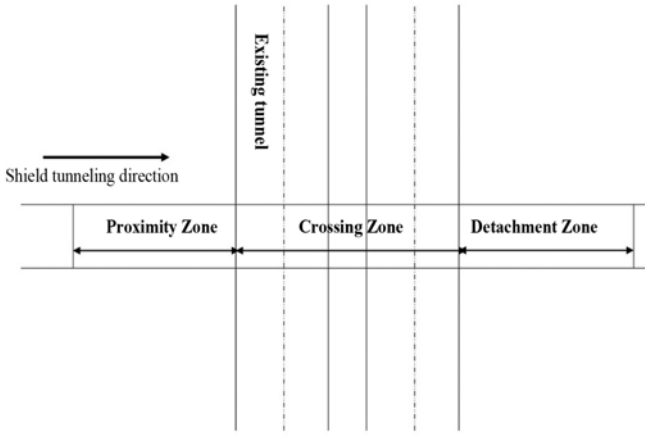

Fig. 7. Plan of the Interaction Zone when Shield Tunnel Crossing the Existing Tunnel

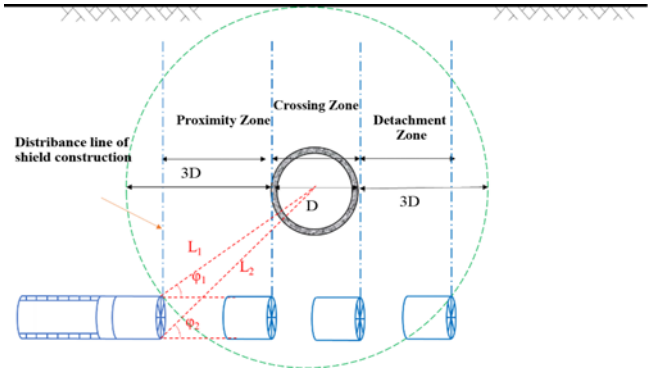

Fig. 8. Sectional Drawing of the Interaction Zone when Shield Undercrossing the Existing Tunnel

In the process of EPB shield under passing existing tunnel, the effect of the existing structure on tunneling thrust is different depending on the disturbing level of soil, which is represented by the change of the earth pressure on the shield machine. Three zones are termed, namely the proximity zone (I zone), crossing zone (II zone) and detachment zone (III zone), as shown in Figs. 7 and 8, and equations for determining the chamber pressure when tunneling machine undercrossing the existing tunnel are proposed.

3.1 Calculation of Chamber Pressure in the Proximity Zone

According to section 2.1 of this paper, excavation of the existing tunnel disturbs the surrounding soil and the range of this disturbance is set as 3 times the excavation diameter D, as shown in Fig. 8. The proximity zone is defined as the zone when the cutter head of the EPB shield is in touch with the disturbance boundary to the cutter head reaches the boundary of the secondary lining structure.

Refer to Fig. 8,

$$L_I = \sqrt{(3.5D)^2 - (c_0 - r)^2}\,. \tag{44}$$

When the shield machine is advancing in the proximity zone, the chamber pressure may be varied since the earth pressure changes due to excavation effect of the existing tunnel. Based on the results provided in section 2.1, the earth pressure above the new tunnel after excavating the existing tunnel may be determined by Eqs. (47) and (48), in which j1 and j2 may be determined by Eqs. (45) and (46):

$$\varphi_1 = arc\tan\frac{c_0 - r}{a};\ L_1 = \sqrt{a^2 + (c_0 - r)^2}\,, \tag{45}$$

$$\varphi_2 = arc\tan\frac{c_0 + r}{a};\ L_2 = \sqrt{a^2 + (c_0 + r)^2}\,, \tag{46}$$

$$q_{e1} = \frac{1}{2}(\sigma_r + \sigma_\varphi) + \frac{1}{2}(\sigma_r + \sigma_\varphi)\cos 2\left(\frac{3}{\pi} - \varphi_1\right) - \tau_{r\theta}\sin 2\left(\frac{3}{2}\pi - \varphi_1\right), \tag{47}$$

$$q_{e2} = \frac{1}{2}(\sigma_r + \sigma_\varphi) + \frac{1}{2}(\sigma_r + \sigma_\varphi)\cos 2\left(\frac{3}{2}\pi - \varphi_2\right) - \tau_{r\theta}\sin 2\left(\frac{3}{2}\pi - \varphi_2\right) + K_0 p_g. \tag{48}$$

3.2 Calculation of Chamber Pressure in the Crossing Zone

When the cutter-head coincides with the boundary of existing lining structure, the removal-and-replacement effect and elastic foundation beam effect should be considered, because these effects induce change of the earth pressure on the shield machine. Based on the results provided in sections 2.1.1, 2.1.3 and 2.2.2, the earth pressures acting on the shield may be determined as follows:

$$q_{e1} = \frac{1}{2}(\sigma_r + \sigma_\varphi) + \frac{1}{2}(\sigma_r + \sigma_\varphi)\cos 2\left(\frac{3}{2}\pi - \varphi_1\right) - \tau_{r\theta}\sin 2\left(\frac{3}{2}\pi - \varphi_1\right) + K_0(p_\Delta - p_z), \tag{49}$$

$$q_{e2} = \frac{1}{2}(\sigma_r + \sigma_\varphi) + \frac{1}{2}(\sigma_r + \sigma_\varphi)\cos 2\left(\frac{3}{2}\pi - \varphi_2\right) - \tau_{r\theta}\sin 2\left(\frac{3}{2}\pi - \varphi_2\right) + K_0(p_\Delta - p_z). \tag{50}$$

3.3 Calculation of Chamber Pressure in the Detachment Zone

As shown in Fig. 8, as the EPB tunnel passes the existing tunnel, the influence of existing tunnel on undercrossing tunnel becomes increasingly small. Therefore, the chamber pressure in this case may be expressed as follows:

$$q_{e1} = \frac{1}{2}(\sigma_r + \sigma_\varphi) + \frac{1}{2}(\sigma_r + \sigma_\varphi)\cos 2\left(\frac{3}{2}\pi - \varphi_1\right) - \tau_{r\theta}\sin 2\left(\frac{3}{2}\pi - \varphi_1\right), \tag{51}$$

$$q_{e2} = \frac{1}{2}(\sigma_r + \sigma_\varphi) + \frac{1}{2}(\sigma_r + \sigma_\varphi)\cos 2\left(\frac{3}{2}\pi - \varphi_1\right) - \tau_{r\theta}\sin 2\left(\frac{3}{2}\pi - \varphi_2\right) + K_0 p_g. \tag{52}$$

4. Verification of the Proposed Method and Discussion

4.1 Case 1

In Xi'an, China, the Metro Line 5 under crosses the Metro Line 2 at the Nanshaomen Station, as shown in Fig. 9. The soil profile

Fig. 9. The Plan View of No. 5 Shield Tunnel Under-Crossing No. 2 Subway in Xi'

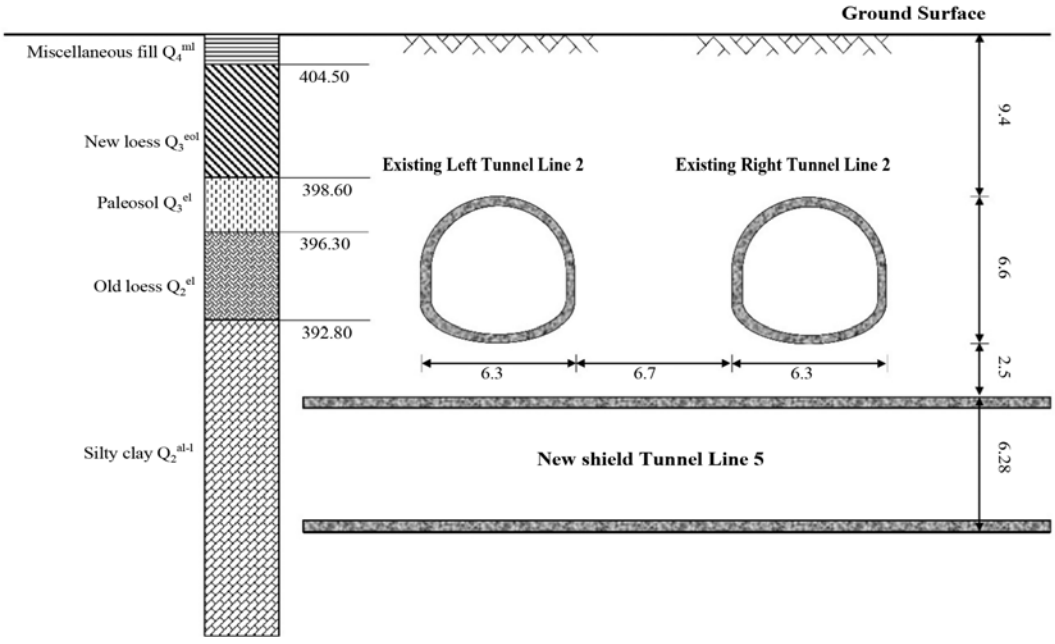

Fig. 10. Profile of No. 5 Shield Tunnel Under-Crossing No. 2 Subway in Xi'an

Table 1. Physico-Mechanical Parameters of Soil in Case 1

Stratum	Buried depth (m)	ρ (g/cm^3)	c (kPa)	φ (°)	μ	G (MPa)	E (MPa)
Miscellaneous fill	0.0 – 1.3	1.73	25	20	0.33	3.5	9.3
New loess	1.3 – 7.2	1.78	35	22	0.32	4.2	10.8
Paleosol	7.2 – 9.5	1.94	40	22	0.31	4.2	11
Old loess	9.5 – 13.4	1.98	40	25	0.31	4.6	12
Silty clay	13.4 – 36	1.99	45	23	0.30	4.6	12

conditions and the spatial locations of the existing tunnel (Metro Line 2) and undercrossing tunnel (Metro Line 5) are shown in Fig. 10. The buried depth of existing tunnel (Metro Line 2) is 9.4 m, and its cross-section width is 6.3 m. C40 concrete was adopted for the lining structure of Metro Line 2 with a thickness of 55 cm. For Metro Line 5, its buried depth is 18.5 m and its outer diameter is 6 m with C50 concrete used as lining structure. The minimum clearance between the existing tunnel and the shield tunnel is about 2.5 m. The properties of soil are shown in Table 1.

According to the Eqs. (45) – (52), the calculation result of the chamber pressure in the process of undercrossing is shown in Fig. 11. Also presented in Fig. 11 is the measured chamber pressure. The tunnel advancing length is measured by the ring number.

It can be seen that the pressure changes in the process of shield tunnel under-crossing the existing tunnel, which can be roughly divided into three stages: 1) As the EPB shield tunnel gradually approaches the existing tunnel, the chamber pressure gradually decreases; 2) in the crossing zone, the chamber pressure reaches the lowest value; 3) in the detachment zone, the chamber pressure gradually increases. Fig. 12 indicates that the

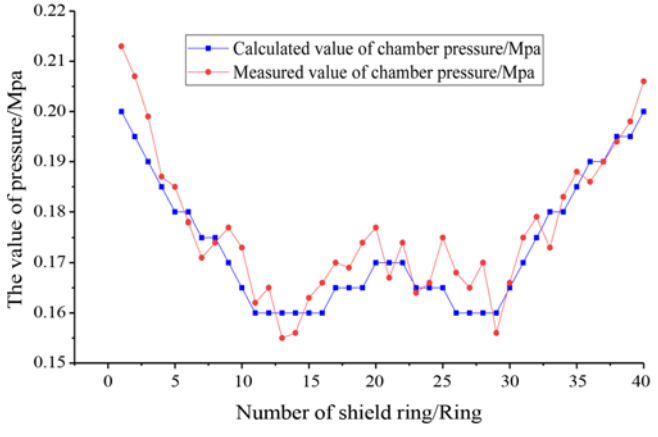

Fig. 11. Comparison between the Calculated Value and the Measured Value of the Chamber Pressure in Case 1

calculated chamber pressure is well agreed with the measure data. At the control nodes (No. 5, No.11 rings, No. 30 rings, and No. 35 rings), the calculated value is approximately equal to the measured value. The average deviation between the calculated value and the measured result is 2.75%, which shows that the

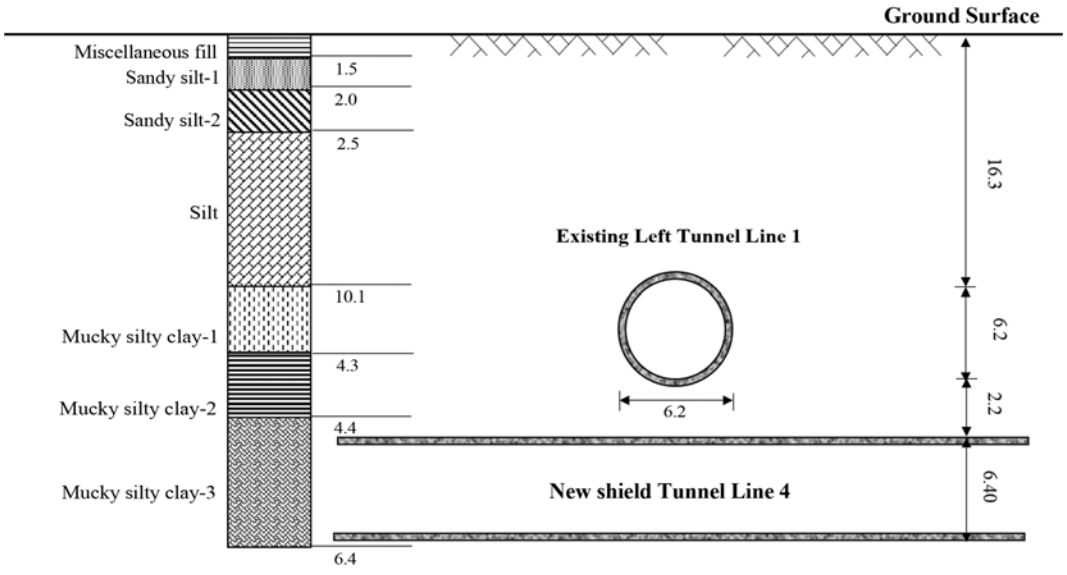

Fig. 12. Profile of No. 4 Shield Tunnel Under-Crossing No. 1 Subway in Hangzhou

Table 2. Physico-Mechanical Parameters of Soil in Case 2

Stratum	Buried depth (m)	ρ (g/cm^3)	c (kPa)	φ (°)	e	K_0
Miscellaneous fill	0.0 – 1.5	1.87	25	30	0.85	0.35
Sandy silt-1	1.5 – 3.5	1.87	0	31.2	0.865	0.36
Sandy silt-2	3.5 – 5.8	1.90	0	32.6	0.785	0.37
Silt	5.8 – 16.9	1.93	0	34.7	0.707	0.36
Mucky silty clay-1	16.9 – 21.2	1.70	12.1	10.6	1.335	0.56
Mucky silty clay-2	21.2 – 25.6	1.75	15.1	10.8	1.151	0.52
Mucky silty clay-3	25.6 – 32	1.81	16	13.9	0.998	0.53

proposed calculation method has high credibility. However, due to superposition of the influence of two existing tunnels and uncertainties in the geological conditions, the deviation between the calculated value and the measured data in the undercrossing zone (15 – 28 rings) is relatively large, reaching 6.01%. It is suggested that the overlapping effect of two existing tunnels can be considered in future work, so as to provide more accurate chamber pressure.

4.2 Case 2

In Hangzhou City, the new shield tunnel of Metro Line 4 is under crossed existing Metro Line 1 as reported by Zhang et al. (2016). As shown in Fig. 12, the buried depth of Metro Line 1 is 16.3 m, and it adopts prefabricated reinforced concrete segment as lining structure with an outer diameter of 6.2 m and an inner diameter of 5.5 m. The undercrossing shield tunnel adopts EPB shield machine for construction with an outer diameter of 6.4 m. The minimum clear distance between the two tunnels is 2.2 m. The soil properties at the site are shown in Table 2.

The comparison between the chamber pressure obtained by the proposed method and the measured results during construction is shown in Fig. 13. Based on comparison results between calculation and actual monitoring, in the overall trend, the calculation results

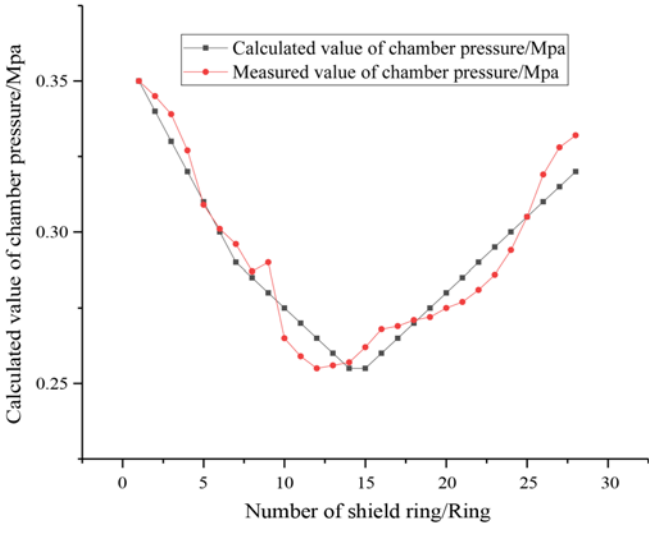

Fig. 13. Comparison between the Calculated Value and the Measured Value of the Chamber Pressure in Case 2

are consistent with the measured values; when EPB shield machine passes through the No.1 interval tunnels, the calculated values are approximately the same as the measured values,

indicating that this method is reasonable and effective setting of the chamber pressure. However, due to the complex mucky silty clay in shield tunneling area in Case 2, and the calculation in this paper is simplified to multi-layer homogeneous soil layer, the deviation between calculated value and measured result still increases to a certain extent (about 2.23%, 2.57%) in some intervals (9 – 17 rings) and (21 – 26 rings). Besides, compared with Case 1, the calculated value of Case 2 is more consistent with the measured value, the average deviation between the calculated value and the measured result is only 1.84%. This may be because the surrounding soil in case 1 has been disturbed more than that in case 2 since there are two existing tunnels in case 1 while only one in case 2. The proposed method is based on elasticity theory, which limits its application in highly disturbed soil.

5. Conclusions

This paper considers the mutual interaction between existing tunnel, surrounding soil and new undercrossing tunneling and proposes a new method for determining the chamber pressure in the process of undercrossing. The main conclusions of this paper are as follows:

1. The effects of existing tunnel on surrounding soil can be identified as removal-and-replacement effect, excavation-induced-disturbance effect, and elastic foundation beam effect. These effects will affect the lateral earth pressure and deformation of soil, which further affect the chamber pressure when shield machine under-crossing the existing tunnel.
2. Based on Mindlin's solution and Winkler's foundation beam theory, this paper deduces equations for calculating the internal force and deformation of existing structure caused by undercrossing shield construction, which is used to reasonably predict the effect of shield construction on the existing subway tunnel during the under-crossing process.
3. Based on analysis of the mutual interaction between existing tunnel and the undercrossing tunneling, the shield tunnel construction area is divided into proximity zone, crossing zone, and detachment zone. When the shield is driving in the proximity zone, the chamber pressure is gradually reduced due to the excavation effect of the existing tunnels. When the shield is driving in crossing zone, the chamber pressure reaches minimum value. When the shield is advancing in detachment zone, the chamber pressure is gradually increased to the original value.
4. Based on the interaction between existing tunnel structure and the EPB shield machine, a new method for calculating the chamber pressure in the undercrossing process is proposed and validated by comparison with measured data from two actual projects. The comparison shows that the proposed method is reasonable with high accuracy.

Acknowledgments

The authors acknowledge the financial support provided by Major Issues of China Railway Corporation (Grant No. 2017G007-G), the National Natural Science Foundation of China (Grant Nos.51378071, 51978064, 51908051), Natural Science Foundation of Shanxi Province (Grant Nos.2014KJXX-53, 2014SZS19-Z01), Natural Science Foundation of Shaanxi Province, China (Grant No. 2018JQ5001), the Fundamental Research Funds for the Central Universities, CHD (Grant Nos.300102219208, 310821163302, 300102210213) and by the Traffic Construction Research Funds of Shanxi Province (Grant Nos. 2016-1-3, 2017-1-4, 2018-1-3).

ORCID

Not Applicable

References

Avgerinos V, Potts DM, Standing JR (2017) Numerical investigation of the effects of tunnelling on existing tunnels. *Géotechnique* 67(9): 808-822, DOI: 10.1680/jgeot.SiP17.P.103

Byun GW, Kim DG, Lee SD (2006) Behavior of the ground in rectangularly crossed area due to tunnel excavation under the existing tunnel. *Tunnelling and Underground Space Technology* 21(3-4), DOI: 10.1016/j.tust.2005.12.178

Chakeri H, Hasanpour R, Hindistan MA, Bahtiyarünver (2011) Analysis of interaction between tunnels in soft ground by 3D numerical modeling. *Bulletin of Engineering Geology and the Environment* 70(3):439-448, DOI: 10.1007/s10064-010-0333-8

Chen H, Lai HP, Qiu YL, Chen R (2019) Reinforcing distressed lining structure of highway tunnel with bonded steel plates: Case study. *Journal of Performance of Constructed Facilities* 34(1):04019082, DOI: 10.1061/(asce)cf.1943-5509.0001363

Chen RP, Li J, Kong LG, Tang LJ (2013) Experimental study on face instability of shield tunnel in sand. *Tunnelling and Underground Space Technology* 33:12-21, DOI: 10.1016/j.tust.2012.08.001

Chen RP, Lin XT, Kang X, Zhong ZQ, Liu Y, Zhang P, Wu HN (2018) Deformation and stress characteristics of existing twin tunnels induced by close distance EPBS under-crossing. *Tunnelling and Underground Space Technology* 82:468-481, DOI: 10.1016/j.tust.2018.08.059

Chen RP, Zhu J, Liu W, Tang XW (2011) Ground movement induced by parallel EPB tunnels in silty soils. *Tunnelling and Underground Space Technology* 26(1):163-171, DOI: 10.1016/j.tust.2010.09.004

Cheng H, Chen J, Chen G (2019) Analysis of ground surface settlement induced by a large EPB shield tunnelling: A case study in Beijing, China. *Environmental Earth Sciences* 78(20), DOI: 10.1007/s12665-019-8620-6

Dimmock PS, Mair RJ (2008) Effect of building stiffness on tunnelling-induced ground movement. *Tunnelling and Underground Space Technology* 23(4):438-450, DOI: 10.1016/j.tust.2007.08.001

Fang YS, Wu CT, Chen SF, Liu C (2014) An estimation of subsurface settlement due to shield tunnelling. *Tunnelling and Underground Space Technology* 44:121-129, DOI: 10.1016/j.tust.2014.07.015

Goh ATC, Zhang W, Zhang Y, Xiao Y, Xiang Y (2016) Determination of earth pressure balance tunnel-related maximum surface settlement: A multivariate adaptive regression splines approach. *Bulletin of*

Engineering Geology and the Environment 77(2):489-500, DOI: 10.1007/s10064-016-0937-8

Huang MS, Zhou XC, Yu J, Leung CF, Jorgin QWT (2019) Estimating the effects of tunnelling on existing jointed pipelines based on Winkler model. *Tunnelling and Underground Space Technology* 86:89-99, DOI: 10.1016/j.tust.2019.01.015

Jin DL, Yuan DJ, Li XG, Zheng HT (2018) Analysis of the settlement of an existing tunnel induced by shield tunnelling underneath. *Tunnelling and Underground Space Technology* 81:209-220, DOI: 10.1016/j.tust.2018.06.035

Kim SH, Burd HJ, Milligan GWE (1998) Model testing of closely spaced tunnels in clay. *Geotechnique* 48(3):375-388, DOI: 10.1680/geot.1998.48.3.375

Lai HP, Zhao X, Kang Z, Chen R (2017) A new method for predicting ground settlement caused by twin-tunneling under-crossing an existing tunnel. *Environmental Earth Sciences* 76(21):1891-1900, DOI: 10.1007/s12665-017-7079-6

Li XG, Chen XS (2012) Using grouting of shield tunneling to reduce settlements of overlying tunnels: Case study in Shenzhen metro construction. *Journal of Construction Engineering and Management - ASCE* 138(4):574-584, DOI: 10.1061/(asce)co.1943-7862.0000455

Li PF, Chen KV, Wang F, Li Z (2019a) An upper-bound analytical model of blow-out for a shallow tunnel in sand considering the partial failure within the face. *Tunnelling and Underground Space Technology* 91: 102989, DOI: 10.1016/j.tust.2019.05.019

Li SH, Li PF, Zhang MJ (2021) Analysis of additional stress for a curved shield tunnel. *Tunnelling and Underground Space Technology* 107: 103675, DOI: 10.1016/j.tust.2020.103675

Li PF, Wang F, Fan LF, Wang HD, Ma GW (2019b) Analytical scrutiny of loosening pressure on deep twin-tunnels in rock formations. *Tunnelling and Underground Space Technology* 83:373-380, DOI: 10.1016/j.tust.2018.10.007

Li PF, Wang F, Zhang CP, Li Z (2019c) Face stability analysis of a shallow tunnel in the saturated and multilayered soils in short-term condition. *Computers and Geotechnics* 107:25-35, DOI: 10.1016/j.compgeo.2018.11.011

Li XG, Yuan DJ (2012) Response of a double-decked metro tunnel to shield driving of twin closely under-crossing tunnels. *Tunnelling and Underground Space Technology* 28:18-30, DOI: 10.1016/j.tust.2011.08.005

Li W, Zhang CP (2020) Face stability analysis for a shield tunnel in anisotropic sands. *International Journal of Geomechanics* 20(5): 04020043, DOI: 10.1061/(ASCE)GM.1943-5622.0001666

Liao SM, Yang JL, Xi CL, Peng FL, Hou XY (2005) Approach to earth balance pressure of shield tunnelling across ultra-near metro tunnel in operation. *Rock and Soil Mechanics* 26(11):1727-1730, DOI: 10.16285/j.rsm.2005.11.007 (in Chinese)

Lin XT, Chen RP, Wu HN, Cheng HZ (2019) Deformation behaviors of existing tunnels caused by shield tunnelling under-crossing with oblique angle. *Tunnelling and Underground Space Technology* 89:78-90, DOI: 10.1016/j.tust.2019.03.021

Liu X, Fang Q, Zhang D, Wang Z (2019) Behaviour of existing tunnel due to new tunnel construction below. *Computers and Geotechnics* 110:71-81, DOI: 10.1016/j.compgeo.2019.02.013

Liu YY, Lai HP (2019) Load characteristics of tunnel lining in flooded loess strata considering loess structure. *Advances in Civil Engineering* 2019, DOI: 10.1155/2019/3731965

Ma J, Li FT, Yuan FF, Zhao Y (2016) Influence on existing tunnel deformation induced by shield. *Railway Engineering* (04):64-67+71 (in Chinese)

Maleki M, Sereshteh H, Mousivand M, Bayat M (2011) An equivalent beam model for the analysis of tunnel-building interaction. *Tunnelling and Underground Space Technology* 26(4):524-533, DOI: 10.1016/j.tust.2011.02.006

Mindlin RD (1936) Force at a point in the interior of a semi-infinite solid. *Physics* 7(5):195-202, DOI: 10.1063/1.1745385

Shi CH, Cao CY, Lei MF (2017) An analysis of the ground deformation caused by shield tunnel construction combining an elastic half-space model and stochastic medium theory. *KSCE Journal of Civil Engineering* 21(7):1933-1944, DOI: 10.1007/s12205-016-0804-y

Shi J, Wang Y, Ng CWW (2016) Three-dimensional centrifuge modeling of ground and pipeline response to tunnel excavation. *Journal of Geotechnical and Geoenvironmental Engineering* 142(11):04016054, DOI: 10.1061/(asce)gt.1943-5606.0001529

Twana KH, Alec MM, Andrea F (2018) Mixed empirical-numerical method for investigating tunnelling effects on structures. *Tunnelling and Underground Space Technology* 73:92-104, DOI: 10.1016/j.tust.2017.12.008

Vesic AB (1961) Bending of beam resting on isotropic elastic solid. *Journal of the Engineering Mechanics Division, ASCE* 87(2):35-53

Wan T, Li PF, Zheng H, Zhang MJ (2019) An analytical model of loosening earth pressure in front of tunnel face for deep-buried shield tunnels in sand. *Computers and Geotechnics* 115:103170, DOI: 10.1016/j.compgeo.2019.103170

Yin ML, Jiang H, Jiang YS, Sun ZY, Wu QL (2018) Effect of the excavation clearance of an under-crossing shield tunnel on existing shield tunnels. *Tunnelling and Underground Space Technology* 78: 245-258, DOI: 10.1016/j.tust.2018.04.034

Yu J, Zhang CR, Huang MS (2013) Soil–pipe interaction due to tunnelling: Assessment of winkler modulus for underground pipelines. *Computers and Geotechnics* 50:17-28, DOI: 10.1016/j.compgeo.2012.12.005

Zhang CP, Han KH, Zhang DL (2015) Face stability analysis of shallow circular tunnels in cohesive–frictional soils. *Tunnelling and Underground Space Technology* 50:345-357, DOI: 10.1016/j.tust.2015.08.007

Zhang ZG, Huang MS (2014) Geotechnical influence on existing subway tunnels induced by multiline tunnelling in Shanghai soft soil. *Computers and Geotechnics* 56:121-132, DOI: 10.1016/j.compgeo.2013.11.008

Zhang CP, Li W, Zhu WJ, Tan ZB (2020) Face stability analysis of a shallow horseshoe-shaped shield tunnel in clay with a linearly increasing shear strength with depth. *Tunnelling and Underground Space Technology* 97:103291, DOI: 10.1016/j.tust.2020.103291

Zhang QF, Xia TD, Ding Z, Huang XB, Lin CG (2016) Effect of nearby undercrossing tunnelling on the deformation of existing metro tunnel and construction control. *Rock and Soil Mechanics* 37(12):3561-3568, DOI: 10.16285/j.rsm.2016.12.027 (in Chinese)

Zhang ZX, Zhang H, Yan JY (2013) A case study on the behavior of shield tunnelling in sandy cobble ground. *Environmental Earth Sciences* 69(6):1891-1900, DOI: 10.1007/s12665-012-2021-4

Zheng HB, Li PF, Ma GW (2021) Stability analysis of the middle soil pillar for asymmetric parallel tunnels by using model testing and numerical simulations. *Tunnelling and Underground Space Technology* 108:103686, DOI: 10.1016/j.tust.2020.103686

Zheng G, Zhang T, Diao Y (2015) Mechanism and countermeasures of preceding tunnel distortion induced by succeeding EPBS tunnelling in close proximity. *Computers and Geotechnics* 66:53-65, DOI: 10.1016/j.compgeo.2015.01.008